EXPERIMENTAL INVESTIGATION OF WEAR PERFORMANCE OF Al7075/ZrO_2/Gr HYBRID METAL MATRIX COMPOSITES USING TOPSIS AND ANN

UDC:66.017:620.17
Original scientific paper https://doi.org/10.46793/adeletters.2025.4.4.4

R. Viswanathan[1], N. Sivashankar[2], P. Muthupandian[3], D. Apparao[4], T. Dinesh[5], R. Thanigaivelan[6*], P. Saravanan[7]

[1] Department of Mechanical Engineering, AVS Engineering College, Salem, Tamilnadu, India
[2] Department of Mechanical Engineering, Kongunadu College of Engineering and Technology (Autonomous), Trichy, Tamilnadu, India
[3] Saveetha Engineering College, Thandalam, Chennai, Tamilnadu, India
[4] Aditya Institute of Technology and Management, Tekkali, Andhra Pradesh, India
[5] Independent Researcher, India
[6] Department of Mechanical Engineering, Shreenivasa Engineering College, Dharmapuri, Tamilnadu, India
[7] Department of Mechanical Engineering, Maha Barathi Engineering College, Chinnasalem, Tamilnadu, India

Abstract:
This study presents the effects of zirconium dioxide (ZrO_2) with 50 nm and graphite (Gr) of 40 µm on the mechanical and tribological behaviour of an aluminium-based metal matrix composite (Al7075) made by stir casting. The tribological behaviour of wear and the frictional qualities of metal matrix composites (MMCs) are further investigated by performing dry sliding wear tests utilising the pin-on-disc method. The TOPSIS Approach was employed to optimise wear parameters such as wear rate (WR) and coefficient of friction (COF). The findings of the analysis of variance demonstrated that the load and incorporation of nanoparticles had a greater influence on WR and COF, respectively. The addition of ZrO_2 results in a significant improvement in wear resistance rate, and COF is significantly reduced with reinforcement of higher wt% ZrO_2. Artificial neural network (ANN) optimisation is performed to check the TOPSIS outcomes and found that the optimal level and its outputs are $P_1V_1D_1M_1$, with WR is 0.00142 mm^3/m and COF is 0.182.

ARTICLE HISTORY
Received: 30 September 2025
Revised: 3 November 2025
Accepted: 19 November 2025
Published: 15 December 2025

KEYWORDS
Aluminum, MMCs, Al7075 alloy, Nano ZrO_2–Gr, TOPSIS, Tribology, ANN

1. INTRODUCTION

Aluminium and its metal matrix composites (AMCs) have shown extreme mechanical and tribological characteristics for various applications such as wear, temperature resistance, etc. Addition of ceramic reinforcements generally enhances the tensile strength, fatigue and stiffness. In terms of tribological behaviour, AMCs show improved wear resistance, reduced coefficient of friction, and better dimensional stability under sliding or abrasive conditions. These enhanced properties arise from the uniform distribution of hard reinforcement particles that resist plastic deformation and minimize material loss during contact, making aluminium composites highly desirable for automotive, aerospace, and structural components [1].

Al7075 is a particular aluminium alloy with strength close to that of steel, excellent corrosion resistance, and a low relative density. These characteristics make Al 7075 useful in the engineering sector [2]. Al7075 has low tribological properties, like all other Al alloys, which prevent it

*CONTACT: R. Thanigaivelan, e-mail: tvelan10@gmail.com

from being used in applications requiring great wear resistance. Methods like mechanical alloying and the creation of MMCs can be utilised to enhance the qualities of an aluminium alloy [3,4]. Composite materials can be manufactured using a variety of methods, including powder metallurgy, squeeze casting, and stir casting. Stir casting is an easy technique that can be utilised for the bulk manufacture of composites. Additionally, the product's price is reduced [5,6]. Different sorts of reinforcing particles are used to create the composites, depending on the application. Due to their increased durability and hardness, ceramic particles are perfect for use as reinforcement particles in particular applications. Hard cermet carbide particles are added to an aluminium alloy to improve its mechanical and tribological properties as well as its hardness at both low and high temperatures [7].

Although ceramics are frequently employed as reinforcement, they greatly lower the composite's ductility while also making it harder and stronger. Some of the ceramic reinforcements utilised with Al 7075 alloy are SiC, Al_2O_3, and ZrO_2 [8,9]. Fly ash was added to the surface of Al 6063, which changed it, and it was discovered that the hardness was increased [10]. The use of self-lubricating powders such as hexagonal BN, graphite and molybdenum disulfide also caught the researcher's attention at the same time. The purpose of using these self-lubricating materials is to reduce the consumption of toxic lubricants as well as energy in industrial components [11]. Girisha and Chittappa [12] investigated the material behaviour of Al356 with zirconium oxide as reinforcement. With the addition of ZrO_2 nanoparticles, improvements in hardness and wear resistance were noted. Nano graphene and ZrO_2 reinforced Al6061 AMCs were investigated and characterised by Satish Babu et al. [13]. ZrO_2 was added to the base alloy of Al 6061, which increased the material's strength and percentage of elongation. To optimise the fabrication parameters as well as the mass fraction levels of reinforcements, material research must be optimised. In material research, both single-objective and multi-objective level optimisation approaches are frequently employed. The most popular optimisation methods employed in recent studies are Principal Component Analysis, TOPSIS, and Grey Relational Grade [14-18]. Sivashankar et al. [19] successfully employed ANN and TOPSIS techniques for accurate prediction of experimental outputs.

Although several studies have investigated aluminium-based metal matrix composites reinforced with ceramic and self-lubricating particles, very limited research has focused on the combined effect of ZrO_2 and Gr reinforcement in Al7075 alloy, particularly in nano-scale proportions. Most existing works have examined either single reinforcement systems (such as Al7075–SiC or Al7075–ZrO_2) or different base alloys (Al6061, Al356) under fixed process parameters. However, the synergistic influence of ZrO_2 and Gr hybrid reinforcements on the tribological and mechanical performance of Al7075 composites remains insufficiently explored. Moreover, there is a lack of systematic optimisation and predictive modelling of stir casting parameters such as load, sliding velocity, and reinforcement fraction using advanced tools like ANN. Therefore, a comprehensive investigation integrating hybrid nano-reinforcement, process optimisation, and ANN-based validation is required to develop high-performance Al7075 composites suitable for automotive tribological applications.

By using ZrO_2 and Gr as reinforcement in a stir casting process, this research aims to create a novel Al7075 aluminium alloy composite and optimise the process variables. ZrO_2 has been chosen as a reinforcement due to its robust, malleable, and ductile characteristics. Due to the improved tribological performance in AMCs, nano reinforcement is recommended [20-22]. Load, sliding velocity, sliding distance, and the combined mass fraction of ZrO_2 and Gr were chosen as input parameters for optimisation. COF and wear rate were considered as output parameters. To validate the test results, an ANN architecture is developed due to its precision and accuracy.

The novelty of this research lies in the development and optimisation of a hybrid Al7075–ZrO_2–Gr nanocomposite fabricated via stir casting, focusing on the combined effect of ceramic and self-lubricating reinforcements. Based on the research gap identified from previous literature, this work is focused on finding the influence of hybrid nano reinforcement on friction and wear rate. In addition to that, the ANN model is implemented to successfully predict the experimental outcomes. This work will enlighten the application of Al7075 and its contributions in various fields, including automotive and aerospace applications.

2. MATERIAL AND METHODS

Al7075 alloy was purchased from Indiamart, with the chemical composition of Al7075 alloy

comprising 5.1–6.1% Zn, 2.1–2.9% Mg, 1.2–2.0% Cu, 0.18–0.28% Cr, ≤0.50% Fe, ≤0.40% Si, ≤0.30% Mn, ≤0.20% Ti, and the remaining percentage being Aluminium (balance). The bottom pouring stir casting machine with the vacuum die casting attachment was used to fabricate the hybrid composites. ZrO_2 and Gr reinforcement particles were mixed with the matrix material Al7075 alloy, using a two-bladed stirrer. As shown in Table 1, three different combined mass fractions of ZrO_2 and Gr were employed to produce hybrid MMC. With the use of an electrical induction heating system and a nitrogen gas inert environment, the Al7075 alloy was first heated to the molten state at 750°C. The mechanical stirring mechanism was put into the molten metal at a constant speed of 500 rpm to provide better turbulence. Furthermore, by adding 1 weight percent of Mg and well stirring, good wettability was attained. ZrO_2 and Gr particles were preheated to 350°C for 30 min before mixing.

An optimised process was used to combine base molten metal with the particles of ZrO_2 and Gr. Finally, composite slurry is injected into the steel die with a graphite coating. The ZrO_2 and Gr nanoparticles are evenly distributed throughout the matrix alloy. The hybrid composite specimen's hardness was then measured using a micro Vickers hardness tester with a 1 kg payload. Al7075 alloy with 3% ZrO_2 + 1%Gr, 2% ZrO_2 + 2%Gr, and 1% ZrO_2 + 3%Gr had hardness values of 178 HV, 185 HV, and 192 HV, respectively.

The hybrid composite specimens were made in a cylindrical shape, each measuring 30 mm in diameter and 300 mm in length. As the central portion of cylindrical composites is typically utilised to evaluate the wear resistance of the composites, the specimens were machined at dimensions suitable for wear tests with a 10 mm diameter and 30 mm length. According to ASTM G99-95, wear tests based on L27 OA were performed in dry conditions with pin-on-disc equipment at room temperature, as shown in Fig. 1. The wear test parameters, which are listed in Table 1, were chosen in accordance with past findings in the literature.

The wear loss of the specimen was measured using an electronic balance with a 0.0001 g precision. Before and after the wear test, each sample was cleaned with acetone to eliminate wear residue. The weight fluctuations that were seen before and after the test revealed the composites' dry sliding wear loss, which was converted into a volume loss. Using Eq. 1, the WR was calculated. Using Eq. 2, the COF was determined. In this, the load cell fixed in the pin-on-disk apparatus is used to determine FT. Table 2 details the experimental outcomes. Each wear and friction test was repeated three times and mean ± SD values are now reported in Table 2.

Fig. 1. Wear test apparatus

$$WR = \frac{V}{S} \quad (1)$$

$$COF = \frac{F_T}{F_N} \quad (2)$$

Where are:
V - Volume loss (mm^3),
S - Sliding Distance (m),
F_T - Tangential force (N),
F_N - Normal force (N).

Table 1. Wear test factors and their range

Parameters	Symbol	Level 1	Level 2	Level 3
Load (N)	P	10	20	30
Sliding velocity (m/s)	V	1	2	3
Sliding Distance (m)	D	400	800	1200
Combined mass fraction of ZrO2− Gr% (wt.%)	M	3% ZrO2+ 1%Gr	2% ZrO2+ 2%Gr	1% ZrO2+ 3%Gr

Table 2. Experimental results with input parameters

S.NO	P	V	D	M	WR	COF
1	10	1	400	1	0.0013	0.187
2	10	1	800	2	0.0021	0.337
3	10	1	1200	3	0.0044	0.502
4	10	2	400	3	0.0030	0.356
5	10	2	800	1	0.0020	0.224
6	10	2	1200	2	0.0025	0.446
7	10	3	400	2	0.0034	0.268
8	10	3	800	3	0.0037	0.434
9	10	3	1200	1	0.0023	0.268
10	20	1	400	2	0.0047	0.359
11	20	1	800	3	0.0036	0.470
12	20	1	1200	1	0.0032	0.349
13	20	2	400	1	0.0028	0.227
14	20	2	800	2	0.0039	0.380
15	20	2	1200	3	0.0057	0.477
16	20	3	400	3	0.0045	0.388
17	20	3	800	1	0.0033	0.247
18	20	3	1200	2	0.0057	0.431
19	30	1	400	3	0.0067	0.514
20	30	1	800	1	0.0042	0.356
21	30	1	1200	2	0.0060	0.452
22	30	2	400	2	0.0059	0.387
23	30	2	800	3	0.0074	0.550
24	30	2	1200	1	0.0059	0.393
25	30	3	400	1	0.0069	0.256
26	30	3	800	2	0.0067	0.425
27	30	3	1200	3	0.0096	0.634

3. RESULTS AND DISCUSSION

3.1 Taguchi Approach

The aim of this effort is to identify the optimal factor levels that offer the lowest possible WR and COF. As a result, a smaller value is preferred, and Eq. (3) provides the expression for determining the signal-to-noise ratio:

$$\mathrm{S/N} = -10 \log \frac{1}{n}\left[\sum_{i=1}^{n} y_i^2\right], \qquad (3)$$

where are:

n – is the number of observations made for this investigation,

y – denotes the outcome of the experiment.

With the use of the Minitab 19 programme, the mean and *S/N* ratio plot was produced.

Fig. 2 provides the mean graphs for the WR. The WR increases as load and sliding velocity increase, presumably due to an increase in the matrix's distortion from the applied stress. It drops slightly at mid-level of the distance, and an increased WR is observed when a decrease in mass fraction of ZrO_2 reinforcement occurs. It represents that ZrO_2 acts as a resistant material and reduces the wear. The ceramic reinforcement significantly affects the reduction in wear rate of MMC. The optimal WR is found at 10 N, 1 m/s, 800 m and 3% ZrO_2 + 1% G. It is noticed that the load has a dominant impact (67.32%) on WR than other parameters.

In comparison to other combinations, 3% ZrO_2 addition results in a higher Hardness value. This is caused by the matrix's increase with nano reinforcement. The hard nanoparticles lead to more resistance to plastic deformation and great hardness. Reducing the size of the reinforcement causes a significant increase in surface area [23]. Additionally, nanoparticle reinforcements dispersed in lubricant formulations have the ability to pass through tiny gaps between two surfaces and alter the tribological characteristics of AMCs [24,25].

Fig. 2. Mean plot for WR

Fig. 3 represents the mean plot for the COF. When the load and distance increase, the COF increases. Meanwhile, when the sliding velocity increases, the COF decreases slightly because the impact between the pin and the disc is low. The friction increases gradually as the percentage of graphite rises due to the self-lubricating qualities of graphite. The mass fraction of ZrO_2 and Gr reinforcement has a major influence on COF. With a reinforcement of 3% ZrO_2 + 1% Gr and a load of 10 N, sliding at a speed of 3 m/s, over a distance of 400 m, the minimum COF was noted. Reinforcement of ZrO_2 + Gr particles has exhibited a dominant influence on COF, followed by distance, applied load and sliding velocity, as observed in the Mean response graph.

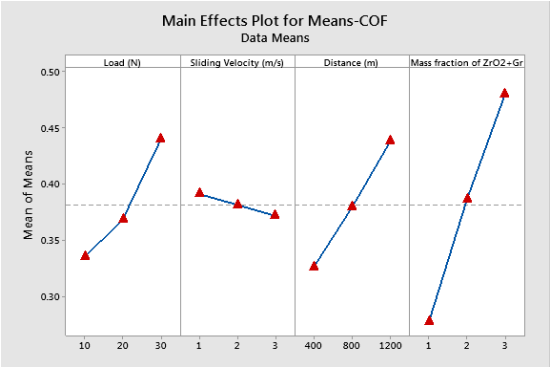

Fig. 3. Mean plot for COF

Eqs. 4 and 5 signify the preferred second-order quadratic models for WR and COF. The results of the WR and COF ANOVA are displayed in Tables 3 and 4, respectively. A higher R^2 value attests to the model's consistency. Predicted R^2 and adj. R^2 values accurately identify improved outcomes. R^2 = 95.09%, R^2 (adj) = 89.36%, and R^2 (Pre) = 74.73% for WR in the ANOVA analysis. R^2 = 97.04%, R^2 (adj) = 93.58%, and R^2 (Pre) = 82.82% for COF. The experimental order demonstrates a high confidence level of the model with 90% confidence and significance, as can be seen from the R^2 values.

Table 3. Analysis of Variance-WR

Source	DF	SS	MS	F	P
Model	14	0.000097	0.000007	16.59	0.000
Linear	4	0.000089	0.000022	53.82	0.000
P	1	0.000067	0.000067	159.98	0.000
V	1	0.000005	0.000005	12.82	0.004
D	1	0.000002	0.000002	4.92	0.047
M	1	0.000016	0.000016	37.56	0.000
Square	4	0.000004	0.000001	2.43	0.104
P*P	1	0.000002	0.000002	3.76	0.076
V*V	1	0.000000	0.000000	0.73	0.410
D*D	1	0.000002	0.000002	5.18	0.042
M*M	1	0.000000	0.000000	0.06	0.805
2-Way Interaction	6	0.000003	0.000001	1.21	0.365
P*V	1	0.000000	0.000000	1.05	0.325
P*D	1	0.000000	0.000000	0.16	0.698
P*M	1	0.000000	0.000000	0.02	0.893
V*D	1	0.000000	0.000000	0.45	0.515
V*M	1	0.000000	0.000000	0.18	0.675
D*M	1	0.000001	0.000001	2.16	0.168
Error	12	0.000005	0.000000		
Total	26	0.000102			

WR=0.00407 - 0.000079 P - 0.00090 V - 0.000008 D + 0.00069 M + 0.000005 P*P + 0.000225 V*V+ 0.000000 D*D - 0.000067 M*M + 0.000022 P*V + 0.000000 P*D + 0.000003 P*M+ 0.000000 V*D - 0.000092 V*M + 0.000001 D*M (4)

COF=0.100 - 0.00004 P - 0.0785 V + 0.000112 D + 0.1068 M + 0.000187 P*P - 0.0001 V*V+ 0.000000 D*D - 0.0077 M*M + 0.000454 P*V - 0.000004 P*D - 0.000112 P*M + 0.000038 V*D+ 0.01462 V*M - 0.000003 D*M (5)

Table 4. Analysis of Variance-COF

Source	DF	SS	MS	F	P
Model	14	0.299390	0.021385	28.09	0.000
Linear	4	0.291524	0.072881	95.73	0.000
P	1	0.049481	0.049481	65.00	0.000
V	1	0.001697	0.001697	2.23	0.161
D	1	0.056476	0.056476	74.19	0.000
M	1	0.183871	0.183871	241.53	0.000
Square	4	0.002494	0.000623	0.82	0.537
P*P	1	0.002094	0.002094	2.75	0.123
V*V	1	0.000000	0.000000	0.00	0.995
D*D	1	0.000049	0.000049	0.06	0.805
M*M	1	0.000351	0.000351	0.46	0.510
2-Way Interaction	6	0.005372	0.000895	1.18	0.380
P*V	1	0.000186	0.000186	0.24	0.630
P*D	1	0.001860	0.001860	2.44	0.144
P*M	1	0.000011	0.000011	0.01	0.905
V*D	1	0.002128	0.002128	2.79	0.120
V*M	1	0.001925	0.001925	2.53	0.138
D*M	1	0.000010	0.000010	0.01	0.912
Error	12	0.009135	0.000761		
Total	26	0.308525			

3.2 TOPSIS Optimization

In this study, the TOPSIS technique is mostly considered to obtain a single optimised response [16]. The decision matrix is the first stage in the TOPSIS approach. Eq. 6 yields the decision matrix (D_{xy}). The weight of each response must be determined in the second stage. By multiplying the decision matrix by its chosen weights, the normalised value of the matrix is calculated in step three. It can be obtained by Eq. 7:

$$D_{xy} = \frac{K_{xy}}{\sqrt{\sum_{i=1}^{m} K_{xy}^2}}, \quad (6)$$

$$A_{xy} = W_i D_{xy}, \quad (7)$$

where are:
D_{xy} - the normalised value,
K_{xy} - the *x-th* value of the *y-th* experimental run,
A_{xy} - Resulting value of matrix element,
W_i - Weight or coefficient of data,
D_{xy} - Input value of position x and y.

Step four involves determining separating measures P+ (Positive Ideal Solution) and P- (Negative Ideal Solution) using Eqs. 8 and 9:

$$P_x^+ = \sqrt{\sum_{i=1}^{n} (A_{xy} - A_y^+)^2}, \quad (8)$$

$$P_x^- = \sqrt{\sum_{i=1}^{n} (A_{xy} - A_y^-)^2}\,, \quad (9)$$

where are:
P_x^+ - Separation distance of the alternative from the positive ideal solution,
A_{xy} - normalized and weighted value,
P_x^- - Separation distance of the alternative from the negative ideal solution,
A_y^+ - Positive Ideal solution,
A_y^- - Negative solution.

The closeness coefficient alternative (CC) is determined in the final phase using Eq. 6. Following the CC evaluation, the Rank is assigned with consideration for the highest CC value. The estimated separation measure values and the alternative coefficient are shown in Table 5 based on Eq. 10:

$$\mathrm{CC}^* = \frac{P_i^-}{P_i^+ + \mathrm{P}_i^-}\,, \quad (10)$$

where are:
P_i^+ - Distance from positive ideal value,
P_i^- - Distance from Negative ideal value.

All parameters are given equal weight when calculating the normalised matrix. Experiment 1 is recommended as the best option, followed by Experiments 5 and 9. This is based on Table 5 – Separation and coefficient options. Experiment 27 is regarded as being of the lowest priority. According to the separation and coefficient alternatives in descending order, the overall preference order is as follows: 1>5>9>13>2>17>7>4>12>6>14>20>8>11>0>16>3>25>22>24>18>15>21>26>19>23>27.

Table 5. TOPSIS Calculations

Normalization		Weighted normalized		Separation measures		CC*
WR	COF	WR	COF	P+	P-	
0.0514	0.0905	0.0172	0.0301	0.00000	0.13044	1.0000
0.0811	0.1633	0.0271	0.0544	0.02619	0.10976	0.8073
0.1740	0.2438	0.0581	0.0812	0.06544	0.07090	0.5200
0.1177	0.1728	0.0393	0.0575	0.03522	0.09741	0.7344
0.0802	0.1085	0.0268	0.0361	0.01132	0.11913	0.9132
0.0982	0.2162	0.0328	0.0720	0.04469	0.09782	0.6864
0.1334	0.1301	0.0445	0.0433	0.03038	0.10045	0.7678
0.1463	0.2107	0.0489	0.0702	0.05104	0.08339	0.6203
0.0902	0.1301	0.0301	0.0433	0.01848	0.11242	0.8588
0.1857	0.1743	0.0620	0.0580	0.05281	0.07768	0.5953
0.1403	0.2279	0.0469	0.0759	0.05454	0.08324	0.6041
0.1255	0.1692	0.0419	0.0563	0.03603	0.09568	0.7264
0.1107	0.1099	0.0370	0.0366	0.02083	0.11052	0.8414
0.1543	0.1842	0.0515	0.0613	0.04641	0.08484	0.6464
0.2235	0.2313	0.0746	0.0770	0.07417	0.05708	0.4349
0.1778	0.1881	0.0594	0.0626	0.05328	0.07738	0.5922
0.1281	0.1197	0.0428	0.0398	0.02740	0.10392	0.7914
0.2249	0.2090	0.0751	0.0696	0.07010	0.06036	0.4627
0.2641	0.2495	0.0882	0.0831	0.08860	0.04223	0.3228
0.1665	0.1726	0.0556	0.0575	0.04716	0.08332	0.6386
0.2367	0.2192	0.0790	0.0730	0.07525	0.05522	0.4232
0.2310	0.1879	0.0772	0.0626	0.06818	0.06286	0.4797
0.2916	0.2667	0.0974	0.0888	0.09939	0.03146	0.2405
0.2310	0.1905	0.0772	0.0634	0.06861	0.06230	0.4759
0.2707	0.1243	0.0904	0.0414	0.07409	0.07053	0.4877
0.2615	0.2061	0.0873	0.0686	0.08003	0.05117	0.3900
0.3766	0.3075	0.1258	0.1024	0.13044	0.00000	0.0000

According to the mean graphs for CC* (Fig. 4), 10 N load (Level 1), 1 m/s Sliding velocity (Level 1), 400 m distance (Level 1) and reinforcement of 3% ZrO_2 + 1% Gr nano particles (Level 1) give the optimal condition for obtaining the lowest WR and COF. The mean and analysis of variance of CC* (Tables 6) show that load has the greatest impact on dry sliding performance characteristics (53.50%), followed by reinforcement of ZrO_2 + Gr particles.

The sliding velocity and distance parameters had no significant effects on the simultaneous optimisation of WR and COF.

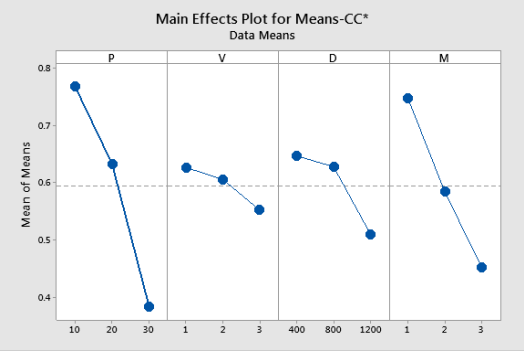

Fig. 4. Mean plot for CC*

Table 6. Analysis of Variance –CC*

Source	DF	Adj SS	Adj MS	F-Value	P-Value	% contribution
P	2	0.68024	0.340119	87.09	0.000	53.50
V	2	0.02626	0.013131	3.36	0.057	2.07
D	2	0.09907	0.049537	12.68	0.000	7.79
M	2	0.39552	0.197761	50.64	0.000	31.11
Error	18	0.07030	0.003905			5.53
Total	26	1.27139				100.00

Validation tests were used to validate the optimised outcomes. The outputs produced at a minimum load of 10 N, a sliding velocity of 1 m/s, a distance of 400 m, and a reinforcement composition of 3% ZrO_2 + 1% Gr were 0.0013 mm^3/m WR and 0.177 COF. ZrO_2 acts as a load-bearing phase, and Gr forms a lubricating film, reducing adhesive wear and coefficient of friction [26].

Figs. 5a and 5b represent the microstructure and worn surface of the specimen. From the Figs. 5a and 5b, it is noted that he predominant wear mechanism observed in the Al7075–ZrO_2–Gr composites is a combination of abrasive and oxidative wear, with the extent depending on the applied load and reinforcement content. The presence of hard ZrO_2 particles strengthens the surface and resists ploughing, thereby reducing severe material removal, while the soft graphite phase acts as a solid lubricant, forming a thin mechanically mixed layer (MML) that stabilizes the contact interface and lowers the coefficient of friction.

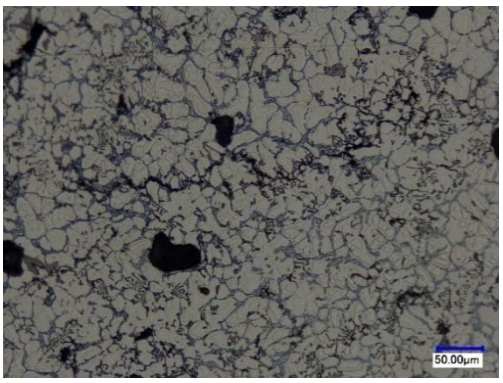

a)

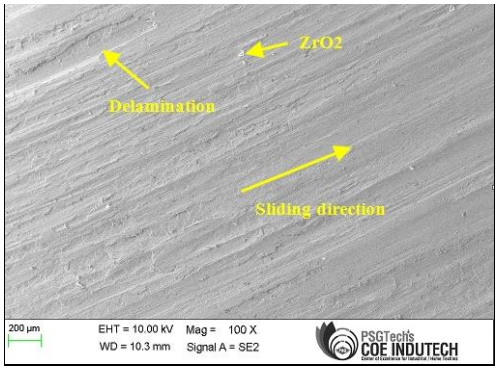

b)

Fig. 5 a) Microstructure of fabricated composites and b) Worn surface at optimal condition

3.3 ANN Technique

ANN architecture is developed with four inputs, ten hidden layers and two output layers (Fig. 6). To train the ANN, initially, a variable is created in MATLAB 15 (Laboratory name: Kongunadu College of Engineering and Technology, Tamil Nadu, India). The TOPSIS experimental is adopted to train the neural network. The input variable is created in MATLAB with 27 experimental combinations and their output is considered the target. The ANN model is trained with 5000 epochs. The performance of the trained ANN model is validated with a gradient curve and a correlation coefficient value. Both curves are generated in MATLAB software and presented in Figs. 7 and 8. The straight line in Fig. 7 gradient curve, indicated the stabilized learning of the ANN model. Fig. 8a indicates the obtained R value of 99.55%. Similarly, from Figs. 8b to 8d, the R value of testing, validation and overall correlation value is noted as 98.5, 97.89 and 98.78%, respectively. Based on ANN results, R=98.78% indicates a strong correlation between inputs and outputs. Based on ANN training, the TOPSIS results are validated and found that the optimal level and its outputs are P1V1D1M1, with WR is 0.00142 mm^3/m and COF is 0.182. The performance of the developed ANN architecture was verified with previous research [27,28].

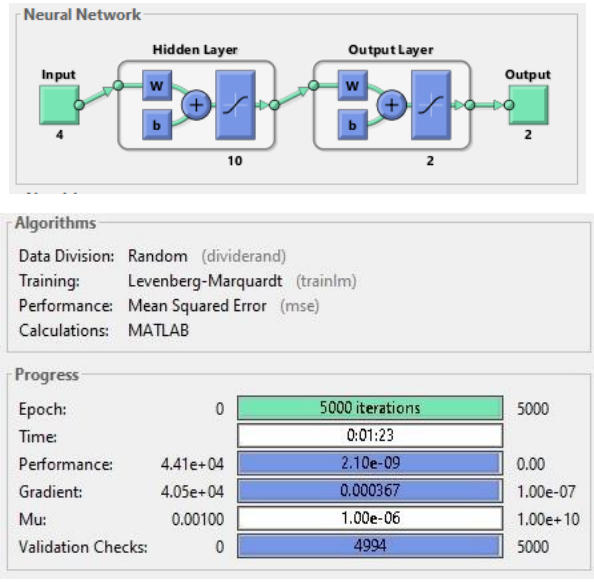

Fig. 6. ANN architecture

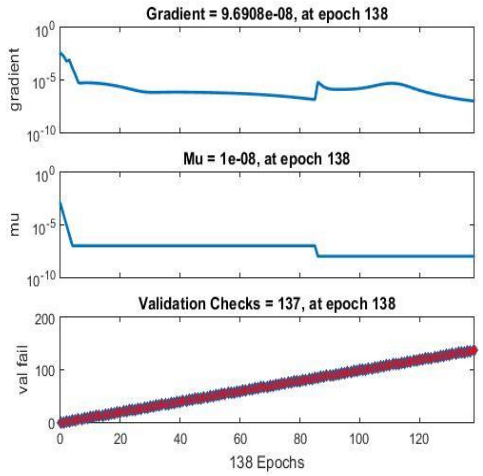

Fig. 7. Gradient Curve

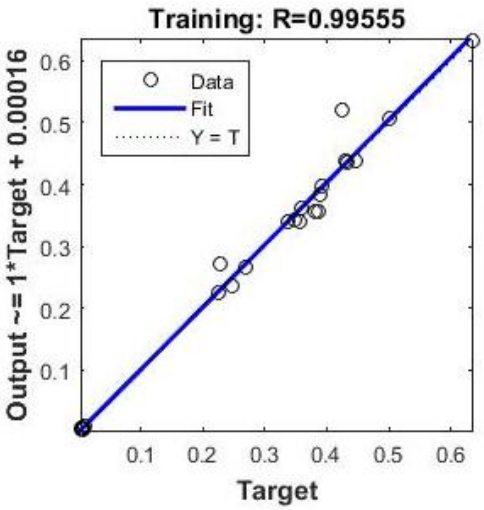

a) R curve - Training

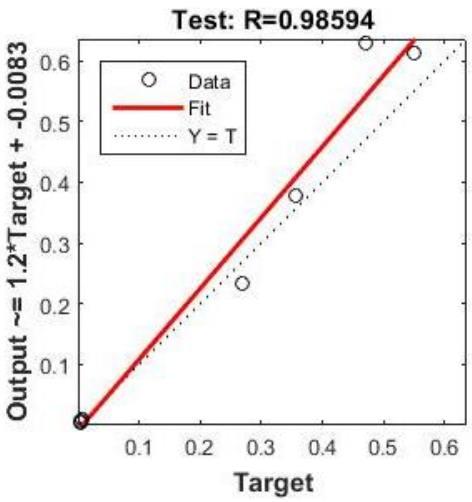

b) R curve - Test

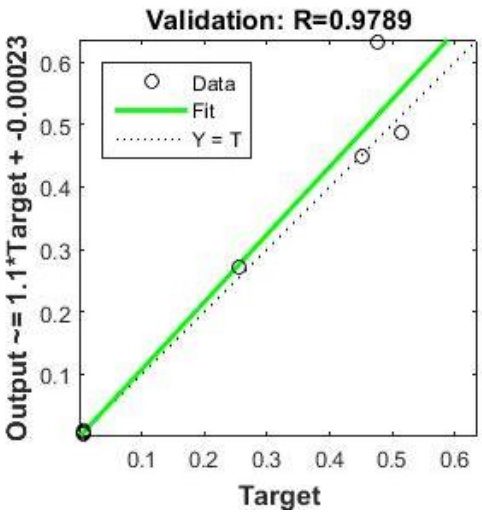

c) R curve – Validation of input

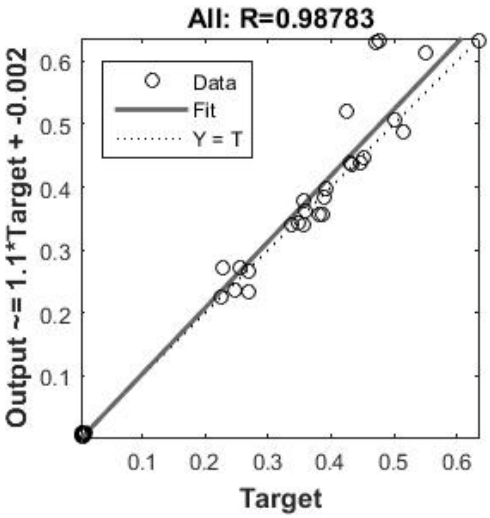

d) Overall R-curve

Fig. 8 (a-d) R-curve

4. CONCLUSION

The current work comprises the manufacturing of Al7075 hybrid composites with varying amounts of ZrO2 and Gr particles, as well as the conduct of wear tests and optimisation of the parameters using the TOPSIS method. The key research results are:

- MMC's mechanical characteristics are improved by the addition of ZrO_2. In contrast, the inclusion of Gr reduces strength while increasing ductility. The addition of ZrO_2 raises the hardness up to 192 HV.
- According to TOPSIS, 10 N load, 1 m/s sliding velocity, 400 m distance, and reinforcement of 3% ZrO_2 + 1% Gr nano particle are the optimal parameters for obtaining the lowest WR and COF.
- Based on ANOVA, load had the greatest impact (67.32%) on WR of the four wear parameters, followed by reinforcement of 3% ZrO_2 + 1% Gr particles, and it was revealed that the addition of ZrO_2 imparted a significant improvement in wear resistance rate.
- According to the ANOVA results, the incorporation of nanoparticles had a dominant influence on COF, and the COF was considerably reduced with the addition of higher wt% of ZrO_2.
- Based on ANN training, the TOPSIS results are validated and found that the optimal level and their outputs are P1V1D1M1 with WR is 0.00142 mm^3/m and COF is 0.182.

CONFLICTS OF INTEREST

The author declares no conflict of interest.

REFERENCES

[1] I. Sudhakar, G. Madhusudhan Reddy, K. Srinivasa Rao, Ballistic behavior of boron carbide reinforced AA7075 aluminium alloy using friction stir processing—an experimental study and analytical approach. *Defence Technology*, 12(1), 2016: 25–31. https://doi.org/10.1016/j.dt.2015.04.005

[2] L. Yu, F. Cao, L. Hou, Y. Jia, H. Shen, H. Li, Z. Ning, D. Xing, J. Sun, The study of preparation process of spray formed 7075/Al–Si bimetallic gradient composite plate. *Journal of Materials Research,* 32, 2017: 3109–3116. https://doi.org/10.1557/jmr.2017.152

[3] X. Liu, M.Q. Zeng, Y. Ma, M. Zhu, Wear behavior of Al-Sn alloys with different distribution of Sn dispersoids manipulated by mechanical alloying and sintering. *Wear*, 265(11-12), 2008: 1857–1863. https://doi.org/10.1016/j.wear.2008.04.050

[4] M.P. Reddy, M. Himyan, F. Ubaid, R.A. Shakoor, M. Vyasaraj, P. Gururaj, M. Yusuf, A.M.A. Mohamed, M. Gupta, Enhancing thermal and mechanical response of aluminum using nanolength scale TiC ceramic reinforcement. *Ceramics International*, 44(8), 2018: 9247–9254. https://doi.org/10.1016/j.ceramint.2018.02.135

[5] J.W. Kaczmar, K. Pietrzak, W. Włosiński, The production and application of metal matrix composite materials. *Journal of Materials Processing Technology*, 106(1-3), 2000: 58–67. https://doi.org/10.1016/S0924-0136(00)00639-7

[6] S. Pardeep, C. Gulshan, S. Neeraj, Production of AMC by stir casting—an overview. *International Journal of Contemporary Practices*, 2(1), 2013: 23–46.

[7] V. Khalili, A. Heidarzadeh, S. Moslemi, L. Fathyunes, Production of Al6061 matrix composites with ZrO_2 ceramic reinforcement using a low-cost stir casting technique: microstructure, mechanical properties, and electrochemical behavior. *Journal of Materials Research and Technology*, 9(6), 2020: 15072–15086. https://doi.org/10.1016/j.jmrt.2020.10.095

[8] G.B.V. Kumar, C.S.P. Rao, N. Selvaraj, M.S. Bhagyashekar, Studies on Al6061-SiC and Al7075-Al_2O_3 metal matrix composites. *Journal of Minerals and Materials Characterization and Engineering*, 9(1), 2010: 43–55. https://doi.org/10.4236/jmmce.2010.91004

[9] S.E. Hernandez-Martinez, J.J. Cruz-Rivera, C.G. Garay-Reyes, C.G. Elias-Alfaro, R. Martínez-Sánchez, J.L. Hernández-Rivera, Application of ball milling in the synthesis of AA7075–ZrO_2 metal matrix nanocomposite. *Powder Technology,* 284, 2015: 40–46. https://doi.org/10.1016/j.powtec.2015.06.030

[10] A. Shanmugasundaram, S. Arul, R. Sellamuthu, Effect of fly ash on the surface hardness of AA6063 using GTA as a heat source. *Metallurgical Research & Technology*, 114(5), 2017: 511. https://doi.org/10.1051/metal/2017053

[11] E. Omrani, A. Dorri Moghadam, P.L. Menezes, P.K. Rohatgi, New emerging self-lubricating metal matrix composites for tribological

applications. In: Ecotribology. Materials Forming, Machining and Tribology. *Springer, Cham,* 2016: 63–103. https://doi.org/10.1007/978-3-319-24007-7_3

[12] K.B. Girisha, H.C. Chittappa, Preparation, characterization and wear study of aluminium alloy (Al 356.1) reinforced with zirconium nanoparticles. *International Journal of Innovative Research in Science, Engineering and Technology,* 2(8), 2013: 3627–3637.

[13] B. Satish Babu, D. Samuel, M.R. Anil Kumar, V. Kumar, T. Aravinda, Synthesis and characterization of nano graphene and ZrO_2 reinforced Al6061 metal matrix composites *Journal of Materials Research and Technology*, 9(4), 2020: 7354–7362. https://doi.org/10.1016/j.jmrt.2020.05.013

[14] N. Sivashankar, R. Viswanathan, K. Periasamy, R. Venkatesh, S. Chandrakumar, Multi-objective optimization of performance characteristics in drilling of Mg AZ61 using twist end mill drill tool. *Materials Today Proceedings*, 37(Part 2), 2021: 214–219. https://doi.org/10.1016/j.matpr.2020.05.033

[15] S. Gajević, A. Marković, S. Milojević, A. Ašonja, L. Ivanović, B.Stojanović, Multi-Objective Optimization of Tribological Characteristics for Aluminum Composite Using Taguchi Grey and TOPSIS Approaches. *Lubricants,* 12(5), 2024: 171. https://doi.org/10.3390/lubricants12050171

[16] R. Arunramnath, P.R. Thyla, N. Mahendrakumar, M. Ramesh, & A. Siddeshwaran, Multi-attribute optimization of end milling epoxy granite composites using TOPSIS. *Materials and Manufacturing Processes,* 34(5), 2019: 530–543. https://doi.org/10.1080/10426914.2019.1566960

[17] M. Pasic, D. Marinkovic, D. Lukic, D. Begic-Hajdarevic, A. Zivkovic, M. Milosevic, K. Muhamedagic, Prediction and optimization of surface roughness and cutting forces in turning process using ANN, SHAP analysis, and hybrid MCDM method. *Applied Sciences*, 14(23), 2024: 11386. https://doi.org/10.3390/app142311386

[18] M.M. Mohan, D. Bandhu, P.V. Mahesh, A. Thakur, U.l Deka, A. Saxena, S. Abdullaev, Machining performance optimization of graphene carbon fiber hybrid composite using TOPSIS-Taguchi approach, *International Journal of Interactive Design and Manufacturing,* 19(1), 2025: 3171–3182. https://doi.org/10.1007/s12008-024-01768-4

[19] N. Sivashankar, R. Thanigaivelan, K.G. Saravanan, Electrochemical micromachining and parameter optimization on AZ31 alloy—ANN and TOPSIS techniques. *Bulletin of the Chemical Society of Ethiopia,* 37(5), 2023: 1263–1273. https://dx.doi.org/10.4314/bcse.v37i5.17

[20] M. Hajizamani, H. Baharvandi, Fabrication and studying the mechanical properties of A356 alloy reinforced with Al_2O_3-10% vol. ZrO_2 nanoparticles through stir casting. *Advances in Materials Physics and Chemistry*, 1(2), 2011: 26–30. https://doi.org/10.4236/ampc.2011.12005

[21] N.G. Yakoub, Effect of nano-zirconia addition on the tribological behavior of Al-7075 Nano composites*. International Journal of Scientific & Technology Research*, 9(08), 2020: 417–421.

[22] K.K. Ekka, S.R. Chauhan, Varun, Dry sliding wear characteristics of SiC and Al_2O_3 nanoparticulate aluminium matrix composite using Taguchi technique. *Arabian Journal for Science and Engineering,* 40, 2014: 571–581. https://doi.org/10.1007/s13369-014-1528-2

[23] A. Kanakaraj, R. Mohan, R. Viswanathan, Parametric optimization of wear parameters on wear rate and coefficient of friction for hybrid (A356 + TiB_2 + ZrO_2) metal matrix composites. *Journal of Ceramic Processing Research,* 23(3), 2022: 268–277. https://doi.org/10.36410/jcpr.2022.23.3.268

[24] J. Umar Mohamed, P.L.K. Palaniappan, P. Maran, R. Pandiyarajan, Influences of ZrO_2 and B_4C reinforcement on metallurgical, mechanical, and tribological properties of AA6082 hybrid composite materials*. Journal of Ceramic Processing Research,* 22(3), 2021: 306–316. https://doi.org/10.36410/jcpr.2021.22.3.306

[25] M.M.B. Mustafa, N. Umehara, T. Tokoroyama, M. Murashima, A. Shibata, Y. Utsumi, H. Moriguchi, Effect of mesh structure of tetrahedral amorphous carbon (ta-C) coating on friction and wear properties under base-oil lubrication condition. *Tribology International*, 147, 2020: 105557. https://doi.org/10.1016/j.triboint.2019.01.016

[26] S.J. Patil, D.P. Patil, A.P. Shrotri, V. Patil, A review on effect of addition of nanoparticles on tribological properties of lubricants. *International Journal of Mechanical*

Engineering and Technology, 5 (11), 2014: 120-129.

[27] S. Miladinović, S. Gajević, S. Savić, I. Miletić, B. Stojanović, A. Vencl, Tribological behaviour of hypereutectic Al–Si composites: A multi-response optimisation approach with ANN and Taguchi–Grey method. *Lubricants*, 12(2), 2024: 61. https://doi.org/10.3390/lubricants12020061

[28] B. Stojanović, R. Tomović, S. Gajević, J. Petrović, S. Miladinović, Tribological behavior of aluminum composites using Taguchi design and ANN. *Advanced Engineering Letters,* 1(1), 2022: 28–34. https://doi.org/10.46793/adeletters.2022.1.1.5

© 2025 by the authors. This work is licensed under a Creative Commons Attribution-Non Commercial 4.0 International License (CC BY-NC 4.0).